MATEC Web of Conferences **33**, 01003 (2015)
DOI: 10.1051/matecconf/20153301003

Martensite and bainite in nanocrystalline steels: understanding, design and applications

Francisca G. Caballero[1,a]
[1]*Spanish National Center for Metallurgical Research (CENIM-CSIC), Avda Gregorio del Amo, 8; Madrid, E-28040, Spain*

Abstract. There are major difficulties in creating novel nanocrystalline structures that have a combination of properties appropriate for large scale applications. An important requirement is to be able to manufacture nanocrystalline components which are large in all dimensions on their macroscale whilst retaining their nanostructure. In addition, the material concerned must be cheap to produce if it is not to be limited to niche applications. Severe plastic deformation has not succeeded in this respect since grain growth cannot effectively be suppressed during consolidation processes. Therefore, processing bulk nanocrystalline materials for structural applications still poses a big challenge, particularly in achieving an industrially viable process. Here we describe various processing strategies and alloy developments currently being explored in the modern steel industry that have the potential to create extremely strong and affordable nanocrystalline engineering steels.

1 Nanocrystalline and nanostructured metals

The term nanometallurgy refers to research in the field of metallurgy, in which at least one critical dimension is in the nanometer regime and significantly influences the behaviour of materials. These dimensions can be external, where typical applications can be found in microelectronics and micro- and nanoelectromechanical systems (MEMS/NEMS) or reflect some important internal length scale like the grain size or the precipitate spacing in alloys.

Metallurgists have been including nanoscale particles into metals for thousands of years: for example, in the strengthening of samurai swords using fine oxide particles as dispersion strengtheners. The fundamental basis for the strengthening of metals using nanoscale particles to impede the movement of dislocations was described by Orowan's strengthening theory in the 1930s.

More recently there has been an interest in developing metals with nanoscale grain structure so-called nanocrystalline metals. A nanocrystalline metal is here defined as a metallic material in which at least one internal length scale is smaller than 100 nm. They contain an exceptionally large density of strong interfaces, rather than only a minor fraction of features such as precipitates, which are small in size. The desire for such materials in the engineering context comes from the expectation of novel mechanical properties, particularly the stress that can safely be tolerated in service.

The method for manufacturing bulk nanocrystalline strong materials is to introduce large numbers of defects such as interfaces or dislocations, which interfere with the ordinary mechanisms of slip or twinning. The defects can be introduced by deformation. Examples include fine nanocrystalline wire with strength in excess of 5 GPa [1]; or metals subjected to equal-channel angular extrusion in which large plastic strains are achieved while maintaining the external shape of the object being deformed. Nanocrystalline metals have yet to establish their technological importance, as the most promising processing routes, namely electro-deposition and severe plastic deformation yield only limited amounts of material.

By contrast, nanostructured metallic materials feature at least one external length scale smaller than 100 nm. With various levels of geometric complexity, this encompasses thin films, nanowires, nanorods and nanoparticles: all of which have potential uses in nano-electronics and nano-electromechanical systems. The strength of crystals increases sharply as they are made smaller. This is because the chances of avoiding defects become greater as the volume of the specimen decreases. In the case of metals, imperfections in the form of dislocations are able to facilitate shearing at much lower stresses than would be the case if whole planes of atoms had to collectively slide across each other. Because defects are very difficult to avoid, the strength in the absence of defects is said to be that of an ideal crystal. For ferritic iron, it follows that the ideal values of tensile and shear strength should be 21 and 11 GPa, respectively.

Nanostructured metals are currently in use and are gaining increasing technological importance as device dimensions are continually being reduced in micro-electronics, sensors and actuators.

[a] Corresponding author: fgc@cenim.csic.es

2 Nanoengineering approach to steel design

In the industry, the term ultra-fine grained is generally used to describe steels with average grain sizes between 1 and 2 μm in diameter and the term submicron (or sub-micrometre) structure to refer to grain sizes between 100 and 1000 nm. Until recently, effective processing techniques to reduce the grain size of these materials to less than 100 nm did not exist.

Combining plastic deformation and phase transformation has been widely used in conventional thermomechanical processing of steels. The most successful example is controlled rolling, with accelerated cooling for plates of low carbon steels. In this process, the target of refinement is the ferrite phase. The mechanisms of the microstructural refinement are recrystallisation of austenite, enhanced nucleation of ferrite from deformed (un-recrystallised) austenite under large supercooling, and inhibition of grain growth of the obtained ferrite. Microalloying with Ti and/or Nb and precise control of rolling conditions (temperature, reduction and pass schedule) have realized a minimum average grain size of 5 μm. Under more severe conditions, the finishing rolling was carried out at a much lower temperature (approximately 500-700ºC). As a result, a 1 μm grain size was achieved on the laboratory scale. Hodgson and co-workers [2] explored the limits of structural refinement in current steels with a ferrite microstructure. In the same context, Seto and Matsuda [3] described the design concepts and properties of already commercialised high strength steel sheets developed by nanoengineering. This work is an extraordinary example of the industrialisation of nano-particle strengthened steels through conventional thermomechanical treatment.

The main drawback of bulk nanocrystalline materials is the lack of both ductility and thermal stability. A practical approach to control instability is to obtain grain structures with a bimodal size distribution, where large grains preferentially accommodate strain and small grains confer high strength such that a combination of high strength and high ductility is obtained as well as significant strain hardening. In this respect, Misra et al. [4] describe the attributes of a promising phase-reversion approach that results in nanometre/ultrafine grain structures in austenitic stainless steels characterised by high strength and high ductility. The approach involves severe cold deformation (45-75%) of metastable austenite to produce martensite, which on annealing for short durations reverts to austenite via diffusional or shear mechanisms, depending on the chemical composition of the steel.

Metallic glasses based on the specialised formulation of ferrous alloys can be used as a precursor to develop a whole range of derived nanoscale structures. These amorphous steels can also be used in the form of powders to produce amorphous/nanocomposite thermally sprayed coatings to enhance the wear and corrosion resistance of engineering components. Branagan et al. [5] provide an overview of the commercial development of bulk materials nanotechnology, which utilises devitrification to expand the process window within which it is possible to achieve nanoscale structure formation in industrial products. In addition, bulk structures consisting of nanoscale precipitates in a glass matrix, produced by spinodal decomposition, are reported to provide significant levels of global plasticity and usable ductility and can undergo deformation without runaway shear propagation. Examples are given of the industrial application of these technologies.

In recent years, novel surface nanocrystallisation approaches have been developed to synthesise nanostructured surface layers on metallic materials by mechanical means, such as by surface mechanical attrition treatment (SMAT) and surface mechanical grinding treatment (SMGT) [6]. With these techniques, microstructures within a surface layer as thick as few hundred micrometres can be effectively refined, forming a nano-grained gradient structure. These treatments provide a simple, flexible and low cost approach to enhance the bulk properties of steels, without any change in the chemical composition.

Table 1. Chemical composition of nanocrystalline bainitic steels, wt.%.

C	Si	Mn	Cr	Mo	V	Nb	Co	Al
1.00	1.53	0.75	0.51	-	-	0.02	-	-
1.01	1.51	0.82	0.46	0.10	-	-	-	-
1.00	1.50	1.90	1.30	0.30	0.10	-	-	-
0.99	1.58	0.76	0.45	-	-	-	-	-
0.98	2.90	0.77	0.45	-	-	-	-	-
0.88	1.54	0.69	0.50	-	-	-	-	-
0.83	1.57	1.98	1.02	0.24	-	-	1.54	-
0.79	1.59	1.94	1.33	0.30	0.11	-	-	-
0.78	1.49	1.95	0.97	0.24	-	-	1.60	0.99
0.67	1.60	1.25	1.50	-	-	-	-	-
0.66	1.45	1.35	1.02	0.24	-	-	-	-
0.64	1.60	1.27	1.50	-	-	0.03	-	-
0.61	1.45	0.76	2.42	-	-	-	-	-
0.58	1.63	1.29	1.43	0.1	-	-	-	-

3 Developing nanocrystalline steels by displacive reaction

In the case of ferritic steels, it is possible to move from ultra-fine to nanoscale by displacive reaction without the use of severe deformation, rapid heat-treatment or mechanical processing. In general, low transformation temperatures are associated with fine microstructures which in turn generally possess both strength and toughness. Following this simple concept, a new generation of steels has been designed in which transformation at low temperature leads to a nanoscale microstructure consisting of extremely fine, 20–40-nm-thick, plates of ferrite and retained austenite [7]. These microstructures are achieved through isothermal transformation to bainite of high carbon high silicon

steels with low martensite start temperature (approx. 120 ºC).

The so-called NANOBAIN steel compositions in Table 1 were defined to decrease bainite transformation temperature, increase the maximum volume fraction of bainite in the final microstructure, and improve the hardenability of the steels. The carbon concentration was selected to suppress the B_S temperature, with the aim of obtaining extremely thin platelets of bainite, and the high silicon content avoids cementite precipitation from austenite during bainite reaction [8]. Cementite is a cleavage and void-initiating phase which is best eliminated from strong steels.

The bainite reaction in first developed nanocrystalline steels steels was found to be extremely slow at low temperatures (between 2 and some 90 days to complete the transformation within the temperature range 125–325ºC) [9]. The transformation was significantly accelerated to complete the processing within hours (as opposed to days), by increasing the magnitude of the driving force for transformation making controlled additions of aluminium and cobalt (Table 1). A further rate increment was possible by reducing carbon, manganese, chromium, and molybdenum contents and by refining the prior austenite grain size with the help of niobium additions [10].

The bainite obtained by low-temperature transformation is harder than ever previously achieved for this microstructure, with values in excess of 700 HV. Tensile strengths above 2 GPa are routinely achieved, with, in one case, an exceptional and unprecedented total elongation of over 20% [11]. Bainite plate thickness and retained austenite content are shown to be important factors in controlling the yield strength, though additional, non-negligible parameters remain to be quantified [12]. Rolling–sliding wear performances are found to be exceptional, with as little as 1% of the specific wear rate of conventional 100Cr6 isothermally transformed to bainite [13]. It is suggested that this results from the decomposition of retained austenite in the worn layer, which considerably increases hardness and presumably introduces compressive residual stresses. Fatigue performance was slightly improved over 100Cr6 for one of the two industrially produced materials, but factors controlling fatigue resistance require further investigation [14].

3.1. Nanoscale and complex structure

Bright field TEM image of nanocrystalline bainite formed at 200 ºC for 240 h in Fe-1.0C-1.5Si-1.9Mn.1.3Cr (wt.%) alloy is presented in Fig. 1. Some of the plates of bainite are incredibly long and thin (20-40 nm), giving an ultra-fine scale structure consisting of an intimate mixture of austenite and ferrite. Plastic relaxation in the austenite adjacent to the bainitic ferrite during bainite reaction may control the final size of the bainitic ferrite plates [15,16]. The defects generated in this process resist the advance of the bainitic ferrite-austenite interface, where the defect density is highest for lower transformation temperatures [17]. Observations revealed that the growth of bainite is accompanied by the formation of dislocations in and around the bainite [18].

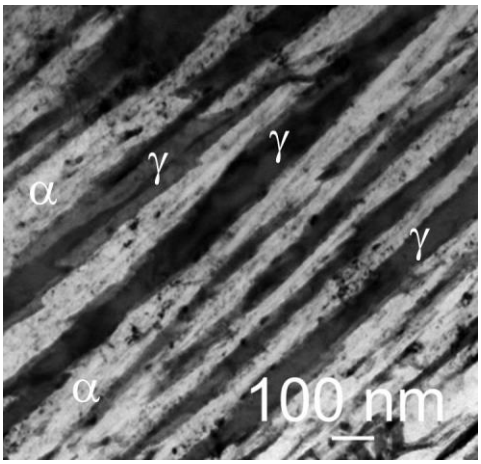

Figure 1. Example of transmission electron micrograph of nanocrystalline bainite formed at 200 ºC for 240 h in Fe-1.0C-1.5Si-1.35Mn.1.3Cr (wt.%) alloy.

Cornide et al. [19] determined the dislocation densities in the bainitic ferrite and austenite phases in nanostructured bainitic steels by TEM to be (5.1 ± 2.7) x 10^{14} m^{-2} and (1.8 ± 0.2) x 10^{14} m^{-2}, respectively. These values are higher than those reported for conventional bainite, 1.7–4.0 x 10^{14} m^{-2} and, in general terms, similar to those measured for martensitic microstructures.

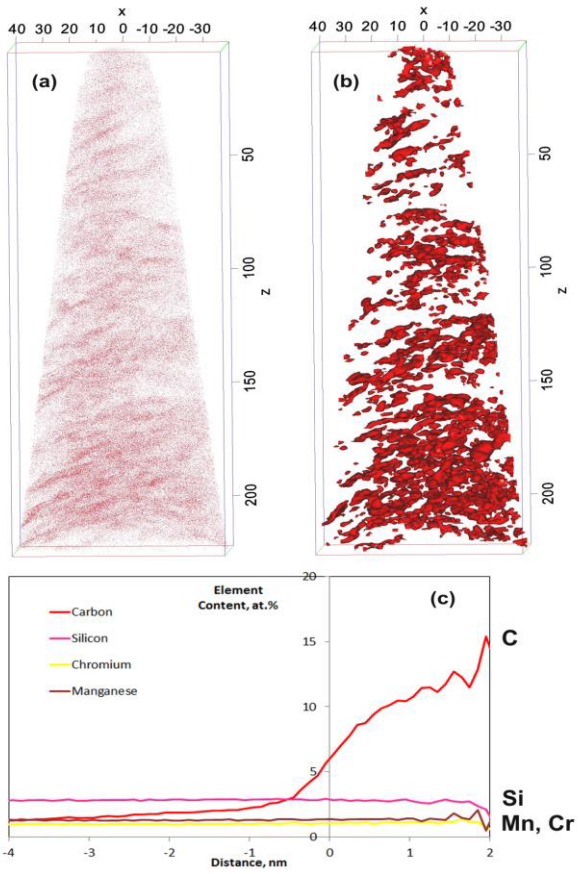

Figure 2. a) Carbon atom map, (b) 5 at.% isoconcentration surfaces and (c) proximity histograms across carbon clusters in nanocrystalline bainite formed at 220 ºC for 240 h in Fe-0.7C-1.44Si-1.6Mn.1.0Cr (wt.%) alloy.

Remarkably, the TEM micrograph shown in Fig. 1 failed to reveal carbide particles inside the bainitic ferrite, leading to the doubtful hypothesis that upper bainite was formed at this extremely low temperature. The presence of cementite, instead ε-carbide, as the lower bainite carbide in nanostructured bainitic steels was later observed by atom probe tomography [20] bellow 350 ºC in nanocrystalline bainite. Likewise, carbon clusters randomly dispersed throughout the bainitic ferrite matrix with a carbon content of 11 at. % and without evidence of substitutional solute partitioning were reported. It is likely that these carbon enriched regions may be associated with carbon segregation to lattice defects and may signify the onset of transitional carbide precipitation [21]. An example of a carbon atom map showing carbon clustering in nanostructure bainitic steels is shown in Fig. 2.

The refinement of the microstructure to the nano-scale is not exclusive of the bainitic ferrite, as retained austenite trapped between the slender plates of ferrite, nano-films, as those shown in Fig. 1 and Fig. 3, also have a size <100 nm. In the past, the term block of austenite has been used to describe unetched surface pools of austenite with sizes of several tens of micrometres trapped between sheaves of bainite. In low-temperature bainitic alloys, the term micro-block is used to denote blocks of retained austenite >1000 nm, and sub-micron blocks those between 100 and 1000 nm.

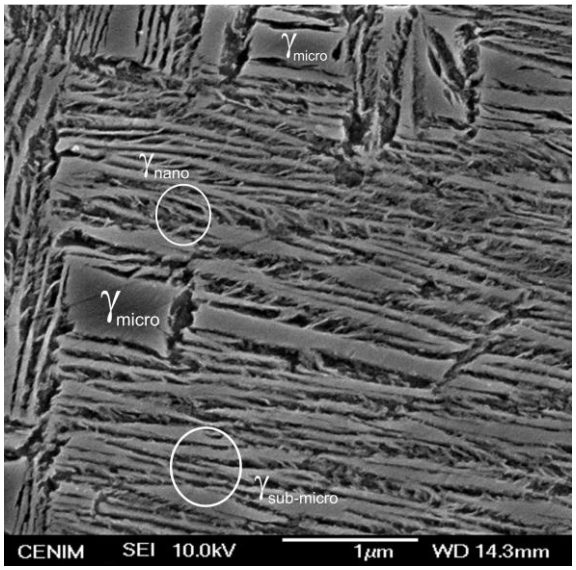

Figure 3. Scanning electron micrograph of nanocrystalline bainite formed at 250 ºC for 40 h in Fe-1.0C-2.9Si-0.8Mn.0.4Cr (wt.%) alloy.

This wide distribution of sizes of the retained austenite in the microstructure, as illustrated in Fig. 3, is expected to result in effective variations of the austenite stability, and to be favourable for spreading the effect of the transformation all along straining and for postponing localization [11]. That is partly because there is a strong correlation between the size of the austenite feature and the amount of C that is retained in solid solution [22], i.e., the smaller the size, the higher the amount of carbon present.

The toughness and fatigue performances of this microstructure is related to the high density of the high angle boundaries that these microstructures usually present [23,14]. This kind of boundary acts as obstacles to cleavage propagation, forcing the cleavage crack to change the microscopic plane of propagation in order to accommodate the new local crystallography. Low angle boundaries are not effective obstacles and, consequently, seem to have no influence on the toughness or fatigue of steels.

The inverse pole figure colour map image in Fig. 4 shows the bainitic structure formed at 250ºC from an austenite grain. The colours correspond to the crystallographic orientation normal to the observed plane, representing different crystallographic variants. The boundaries were drawn where the misorientation angle is greater than 10º. The corresponding pole figure shows some orientation scattering from the ideal N–W orientation relationship. The ideal N–W orientations of the 12 variants are rotated to coincide with the actual {011} pole figure of the measured transformed bainite. Then each variant was accordingly identified on the orientation map. It is revealed that a prior austenite grain was divided by packets consisting of three blocks of which the orientations are entirely different to each other. Each block contains a single variant of the bainitic lath.

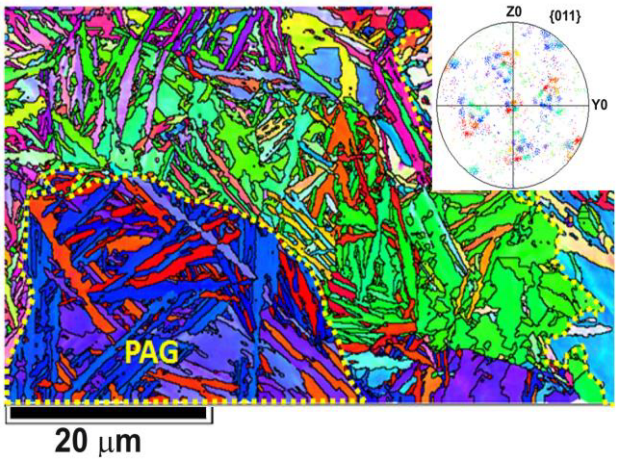

Figure 4. The inverse pole figure of nanocrystalline bainite formed at 250 ºC for 16 h in Fe-0.7C-1.6Si-1.2Mn.1.5Cr (wt.%) alloy, and corresponding {011} pole figure representing orientations of bainite laths. The black thin line represents the misorientation angles greater than 10º and the dashed yellow, coarse line represents selected prior austenite grain boundaries.

3.2. Tetragonal and carbon super-saturated ferrite

In addition, atom probe tomography revealed significant amounts of carbon in bainitic ferrite, which are over ten times above that expected from PE phase boundaries [24,25]. Efforts to understand the excess in carbon in the ferritic lattice are mainly focused in two directions; first, a change in symmetry from the conventional cubic unit cell into a tetragonal lattice, and second, the presence of a high density of defects, particularly vacancies.

Table 2. Result of Rietveld X-ray diffraction pattern refinement as a function of the bainite transformation temperature

Temperature (ºC)	*a* (nm) ±0.0001	*c* (nm) ±0.0001	*c*/*a*
220	0.2856	0.2880	1.0084
220(+6d)	0.2855	0.2879	1.0084
250	0.2856	0.2878	1.0077
300	0.2857	0.2877	1.0070
350	0.2859	0.2876	1.0059
As quenched	0.2856	0.2932	1.0266

Regarding the tetragonality of bainitic ferrite, there are numerous experimental indications so far, evidenced by well-developed techniques, such as X-ray diffraction, high resolution transmission electron microscopy [26], and synchrotron radiation [27] that revealed a shift in the c/a parameters (see Table 2) caused by the presence of carbon that changes the equilibrium between austenite and ferrite.

On the other hand, vacancies contribute to the transport of substitutional atoms during bainitic transformation and are as well utilized by interstitial solute atoms to flatten their pile-up in the parent phase near the advancing boundary [28]. Specific interstitial lattice sites near the defects in bainitic ferrite provide lower-energy sites for carbon than the regular interstitial lattice positions because of the stress field around these defects. Meanwhile, the ease in formation of the vacancy-carbon pair or complex by the motion of carbon and vacancy under irradiation, deformation, or quenching has been proven theoretically and experimentally in the Fe-C system [29-32].

3.3. Industrialization of nanocrystalline bainitic steels

Two different industrial component demonstrators were tested in their representative conditions. First, a Fe-0.6C-1.6Si-1.25Mn-1.75Cr (wt.%) industrial grade transformed at 270ºC was used to manufacture a metal scrap shear of 524x80x200 mm^3 dimensions. The standard material for this application normally provides 8000-12000 cuts over their lifetime. The number of cuts achieved with the nanocrystalline blade was lower though of similar order of magnitude. Overall, it is believed that wear performance should undoubtedly be on par with the standard material once some fine tuning is carried out. Despite the potential added cost due to the thermal treatment, gross benefit is estimated to be 10-20% due to the significantly cheaper material.

In addition, the potential for industrial application in high loaded diesel injection systems was evaluated using so-called technological demonstrators with both, the Fe-0.6C-1.6Si-1.25Mn-1.75Cr (wt.%) and Fe-1C-2.5Si-0.75Mn-1Cr (wt.%) industrial grades transformed at 250 ºC. The specimen used for these tests had the same characteristic bore intersection as a rail body. Internal pulsating tests were carried out at a stress ratio R=0.1. While results obtained on nanocrystalline bainitic steel containing 1.0 wt.% C were well below expectations, most likely due to the relatively poor cleanliness of the material, results obtained on that containing 0.6 wt.% C were on par with those obtained on 100Cr6 commercial steels in spite of the significantly lower ultimate tensile strength of the nanocrystalline steel. Because fatigue properties were difficult to correlate to microstructure, it is expected that further improvement can be made over this first set of results, once the contributing factors are better understood and quantified.

Summary

Solid state reactions can be used to refine the structure scale in steels and to accomplish phase sizes in the nanoscale regime. This achievement represents an enabling ability to develop vastly improved properties which are not possible on conventional length scales.

References

1. H.K.D.H. Bhadeshia, H. Harada, Appl Surf Sci **67**, 326 (1993).
2. H. Beladi, I.B. Timokhina, X.Y. Xiong, P.D. Hodgson, Acta Mater **61**, 7240 (2013).
3. K. Seto, H. Matsuda, Mater Sci Technol **29**, 1158 (2013).
4. R.D.K. Misra, Z. Zhang, P.K.C. Venkatasurya, M.C. Somani, L.P. Karjalainen, Mater Sci Eng **A527**, 7779 (2010).
5. D.J. Branagan, A.V. Sergueeva, S. Cheng, J.K. Walleser, T.F. Weznel, J.V. Costa, W. Kiilunen, B.E. Meacham, C.D. Tuffile, Mater Sci Technol **29**, 1193 (2013).
6. T. Roland, D. Retraint, K. Lu, J. Lu, Mater Sci Eng **445-446**, 281 (2007).
7. F.G. Caballero, C. Garcia-Mateo, M.K. Miller, JOM **66**, 747 (2014).
8. F.G. Caballero, H.K.D.H. Bhadeshia, Curr Opin Solid State Mater Sci **8**, 251 (2004).
9. C. Garcia-Mateo, F.G. Caballero, H.K.D.H. Bhadeshia, ISIJ Int **43**, 1238 (2003).
10. T. Sourmail, F.G. Caballero, C. Garcia-Mateo, V. Smanio, C. Ziegler, M. Kuntz, R. Elvira, A. Leiro, E. Vuorinen, T. Teeri, Mater Sci Technol **29**, 1166 (2013).
11. C. Garcia-Mateo, F.G. Caballero, T. Sourmail, M. Kuntz, J. Cornide, V. Smanio, R. Elvira, Mater Sci Eng **A549**, 185 (2012).
12. S.S. Babu, S. Vogel, C. Garcia-Mateo, B. Clausen, L. Morales-Rivas, F.G. Caballero, Scr Mater **69**, 777 (2013).
13. A. Leiro, E. Vuorinen, K.G. Sundin, B. Prakash, T. Sourmail, V. Smanio, F.G. Caballero, C. Garcia-Mateo, R. Elvira, Wear **298**, 42 (2013).
14. R. Rementeria, L. Morales, M. Kuntz, C. Garcia-Mateo, E. Kerscher, T. Sourmail, F.G. Caballero, Mater Sci Eng **A630**, 71 (2015).
15. L.C. Chang, H.K.D.H. Bhadeshia, Mater Sci Technol **11**, 105 (1995).
16. J. Cornide, C. Garcia-Mateo, C. Capdevila, F.G. Caballero, J Alloys Compd **577S**, S43 (2013).

17. M.K. Fondekar, A.M. Rao, A.K. Mallik, Metall Trans A **1**, 885 (1970).
18. F.G. Caballero, Hung-Wei Yen, M.K. Miller, Jer-Ren Yang, J. Cornide, C. Garcia-Mateo, Acta Mater **59**, 6117 (2011).
19. J. Cornide, G. Miyamoto, F.G. Caballero, T. Furuhara, M.K. Miller, C. Garcia-Mateo, Solid State Phenom **172-174**, 117 (2011).
20. F.G. Caballero, M.K. Miller, C. Garcia-Mateo, Mater Chem Phys **146**, 50 (2014).
21. F.G. Caballero, M.K. Miller, C. Garcia-Mateo, Metall Trans A **42**, 3660 (2011).
22. C. Garcia-Mateo, F.G. Caballero, M.K. Miller, J.A. Jiménez, J Mater Sci **47,** 1004 (2012).
23. F.G. Caballero, H. Roelofs, St. Hasler, C. Capdevila, J. Chao, J. Cornide, C. Garcia-Mateo, Mater Sci Technol **28**, 95 (2012).
24. F.G. Caballero, M.K. Miller, C. Garcia-Mateo, Acta Mater **58**, 2338 (2010).
25. F.G. Caballero, M.K. Miller, C. Garcia-Mateo, J. Cornide, M.J. Santofimia, Scr Mater **67**, 846 (2012).
26. C. Garcia-Mateo, J.A. Jimenez, H-W Yen, M. K. Miller, L. Morales-Rivas, M. Kuntz, S.P. Ringer, J-R Yang, F.G. Caballero, Acta Mater **91**, 162 (2015).
27. C.N. Hulme-Smith, I. Lonardelli, A.C. Dippel, H.K.D.H. Bhadeshia, Scr Mater **69**, 409 (2013).
28. S. van der Zwaag, J.A. Wang, Scr Mater **47,** 169 (2002).
29. P. Hautojärvi, J. Johansson, A. Vehanen, J. Yli-Kauppila, P. Moser, Phys Rev Lett **44,** 1326 (1980).
30. O. Seydel, G. Frohberg, H. Wever, Phys Status Solidi A **144**, 69 (1994).
31. D. Terentyev, N. Anento, A. Serra, V. Jansson, H. Khater, G. Bonny, J Nucl Mater 408, **272** (2011).
32. G.A. Nematollahi, J. von Pezold, J. Neugebauer, D. Raabe, Acta Mater **61**, 1773 (2013).